Supplemental materials for

# Rectified activity-dependent population plasticity implicates cortical adaptation for memory and cognitive functions

Hong Xie[1,2*#], Kaiyuan Liu[3,4*], Dong Li[5*], Chang-Shui Zhang[6,7], Claus C. Hilgetag[5], Ji-Song Guan[3,8#]

1. School of Artificial Intelligence Science and Technology, University of Shanghai for Science and Technology, 200093, Shanghai, China.
2. Institute of Photonic Chips, University of Shanghai for Science and Technology, 200093, Shanghai, China.
3. School of Life Science and Technology, Shanghai Tech University, 201210, Shanghai, China.
4. School of Life Sciences, Tsinghua University, 100084, Beijing, China.
5. Institut für Computational Neuroscience, Universitätsklinikum Hamburg-Eppendorf, Martinistr. 52, 20246 Hamburg, Germany
6. Department of Automation, Tsinghua University
7. State Key Lab of Intelligent Technologies and Systems, Tsinghua National Laboratory for Information Science and Technology (TNList) Beijing 100084, P.R.China
8. State Key Laboratory of Advanced Medical Materials and Devices, ShanghaiTech University, Shanghai, China
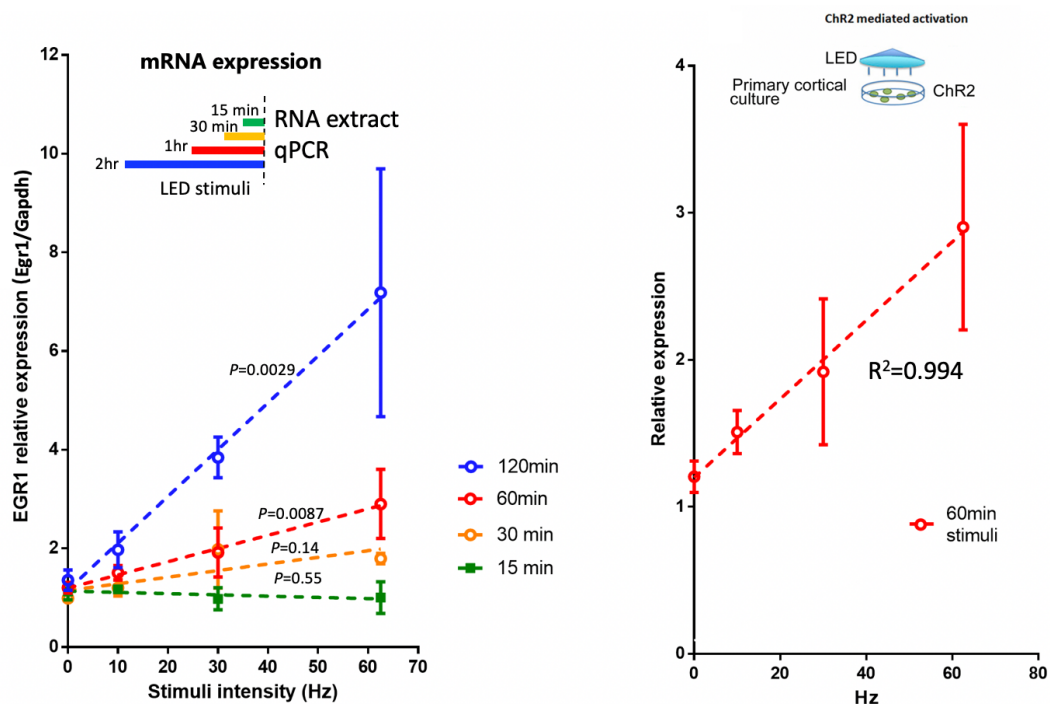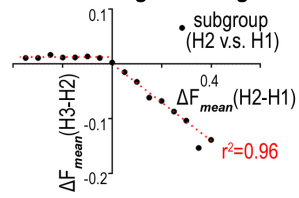
**Supplementary Figure 1. Linear correlation between EGR1 expression and neural activity in cultured neurons**

**Left.** qPCR measurement of the correlation between light-induced activity and endogenous egr1 gene expression level. ChR2-mCherry–expressing neurons were stimulated continuously with LED (~480 nm, 5-ms duration for each pulse) at the indicated frequencies. Neurons were harvested at the indicated time points. Three replicates were measured in each experiment. Three identical experiments and 9 biological samples were measured for each data point. The mean values of each experiment were used for the statistics. P value is for test in linear regression as slope significant non-zero. **Right.** Frequency dependency of the Egr1-EGFP transcription in cultured neurons with continuous optical stimuli for 1 hour. Data were gathered as described in left. $r^2=0.994$. Error bars indicate SEM.

**A** *mean of signal changes in later trial (VISam)*

subgroup (H2 v.s. H1)

$\Delta F_{mean}$(H2-H1)

$r^2=0.96$

$\Delta F_{mean}$(H3-H2)

**B** *Deviation of signal changes in later trial*

$r^2=0.95$
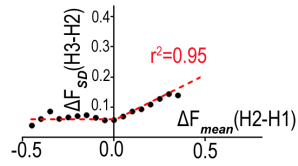
$\Delta F_{mean}$(H2-H1)

$\Delta F_{SD}$(H3-H2)

Figure S2

**Supplementary Figure 2. Example of the activity-dependent population plasticity in one volume**

Rectified linear correlation between prior and posterior changes of each subgroup in for the mean activity (**A**), or the standard deviation of the activity (**B**). Each dot represents a subgroup of more than 200 neurons of area VISam. One representative volume shown.

**A**
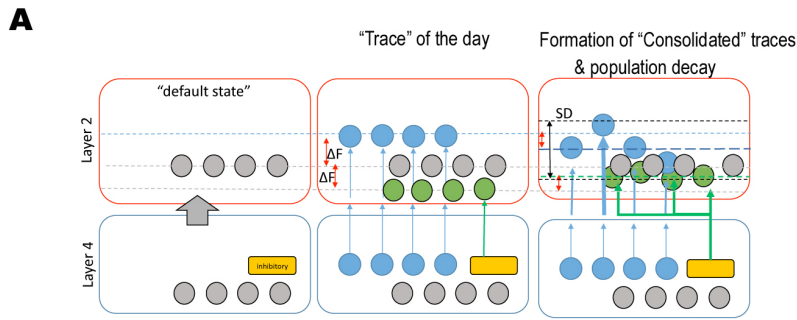


**B**

$$\Delta S_2^{Amp.} = \begin{cases} -0.34 \cdot \Delta S_1^{Amp.}, & \Delta F_1 > -0.05 \\ 0.013, & \Delta F_1 < -0.05 \end{cases}$$

$$\Delta S_2^{s.d.} = \begin{cases} 0.21 \cdot \Delta S_1^{Amp.} + 0.05, & \Delta F_1 > -0.05 \\ -0.07 \cdot \Delta S_1^{Amp.} + 0.05, & \Delta F_1 < -0.05 \end{cases}$$

**Supplementary Figure 3. Description of state changes under activity-dependent cortical variability.**

**A.** The scheme summarizes the activity dynamics of activity-dependent cortical variability.

**B.** Formulation for the state changes of population activity. The population activity changes in the posterior trial ($\Delta S_2$) are determined by the activity changes in the prior trial ($\Delta S_1$). Parameters were averaged from 18 individuals (Figure 1G&H). Amp., amplitude, ($\Delta F_{mean}$); s.d., variation, ($\Delta F_{s.d}$).
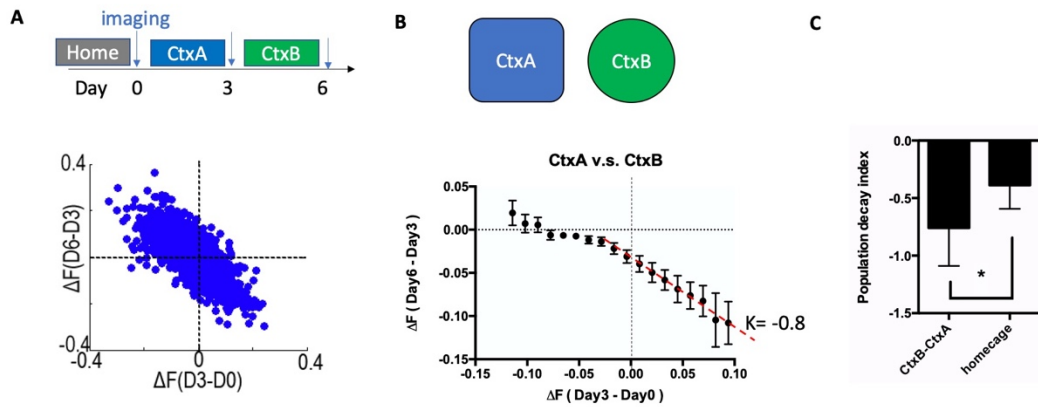
**Supplementary Figure 4. Distinct sensory inputs yield a near -1 slope**
Mice were put in context A (square floor) or context B (round shape arena) for 30 minutes and imaged at 1 hour after the end of each training section on day 3 and day 6. **A**. One example of the EGR1-EGFP signal changes; **B**. Signal alternations in Day 6 v.s. Day 3 in each subgroup of neurons, which are divided by signal alternation between Day3 and Day0. (N=4 mice). Error bar, SEM. **C**. Comparing between the population decay index of distinct contexts and homecage trials. *, $p < 0.05$. student *t*-test. Error bars indicate SEM.
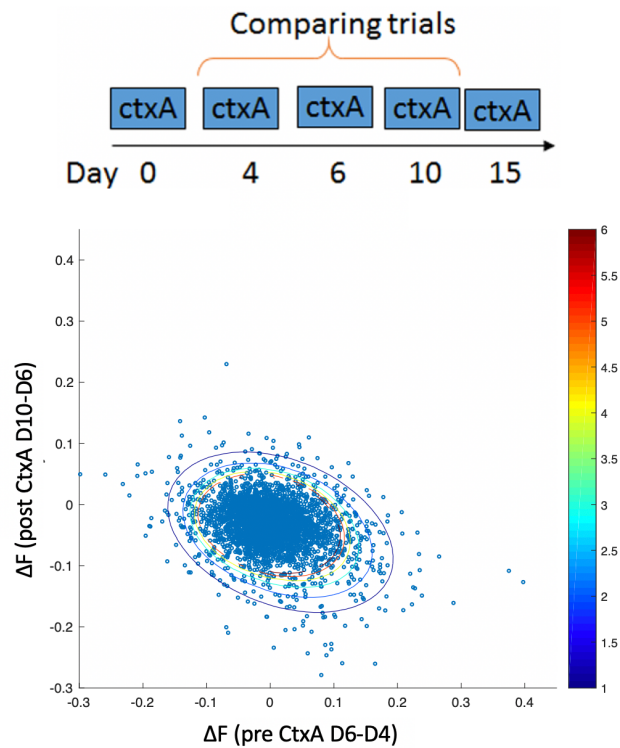
**Supplementary Figure 5  The population plasticity in trials of a neutral context (CtxA)**

Activity change correlation between the earlier versus later trials in the neutral environment (CtxA) for cortical layer 2/3 neurons. Color-coded contour lines plot the gradient of normal distribution.
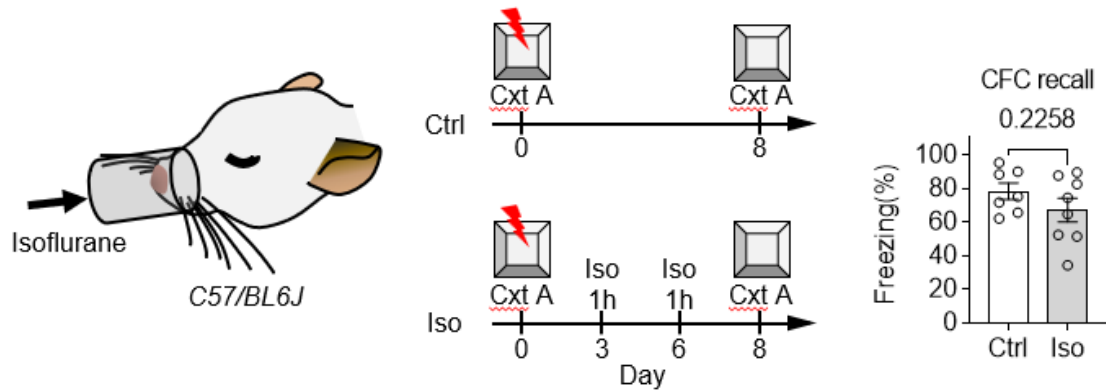
**Supplementary Figure 6. The effect of isoflurane induced anesthetize procedure did not affect memory retrieval several days later**

Two groups of mice were trained in context A box for fear conditioning test. Control group(n=7) was tested directly on day 8 in context A. Iso group mice(n=8) were treated with isoflurane for 1 hour, mimicking the imaging conditions on day 3 and day 6. On day 8 mice were placed in context A for fear memory recall. Error bar, SEM.
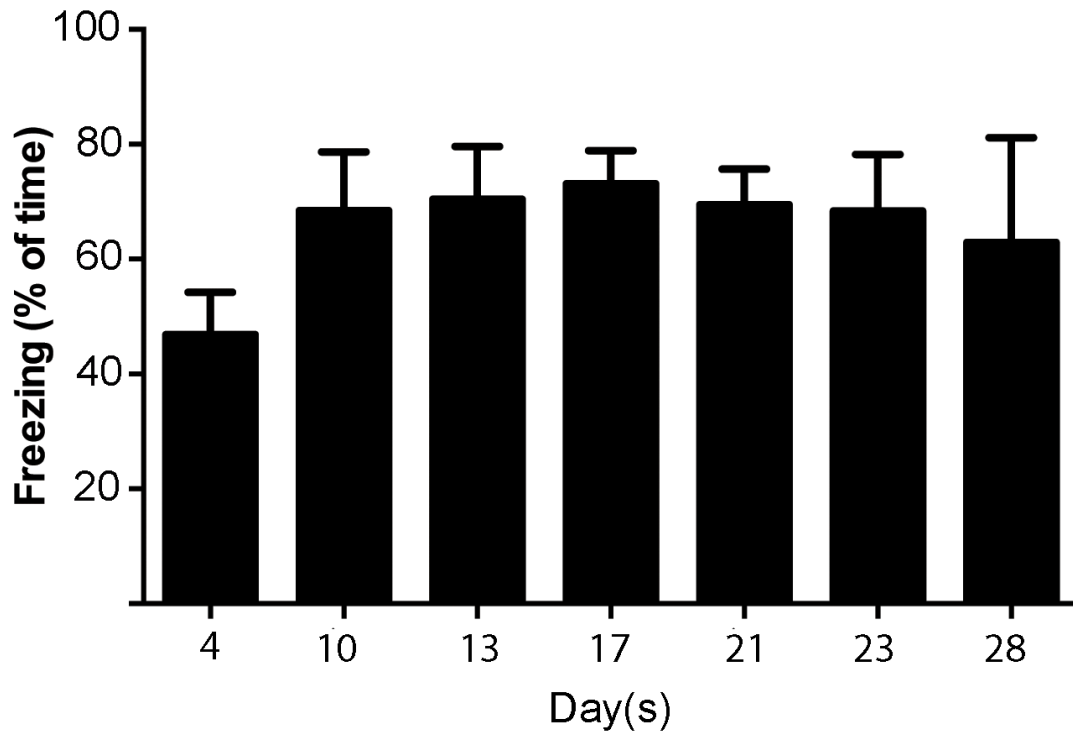
**Supplementary Figure 7. The freezing levels in the recall trials (related to figure 2D)**

A group of Egr1-EGFP mice (n=6) were subjected to contextual fear conditioning training and two-photon imaging. The freezing levels showed trends of steady memory retrieval in those mice. Error bar, SEM.
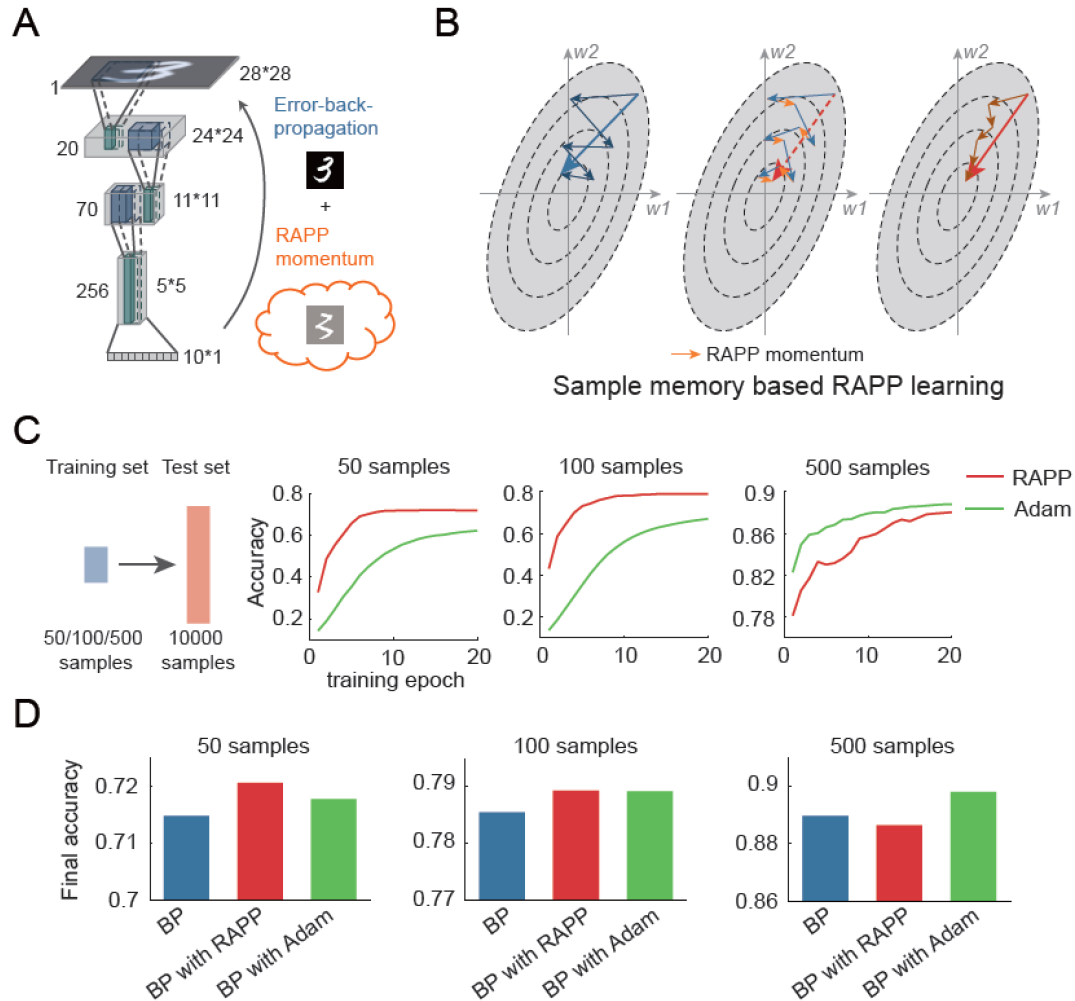
**Supplementary Figure 8. Learning with RAPP rule in CNN results in high efficiency and accuracy in MNIST handwritten digit classification task with small sample size.** (**A**) A well-described CNN structure. There are 4 convolutional layers with kernel sizes=[5,4,3,5] and the number of channels=[20,70,256,10]. All of the optimizers were trained on the same CNN structure. (**B**) The illustration of RAPP rule in momentum of each BP step. The blue line shows the BP training process and the orange line shows the RAPP training process. (**C** and **D**) Accuracy results on few-shot tasks. The test accuracy of first 20 epochs (C) and the final test accuracy (200 epochs for 5/10 training samples per category and 400 epochs for 50 training samples per category) (D) for each optimizer is shown. Learning speed and other parameters are tuned to meet the highest accuracy for Adam.